Analytical Methods

Accepted Manuscript

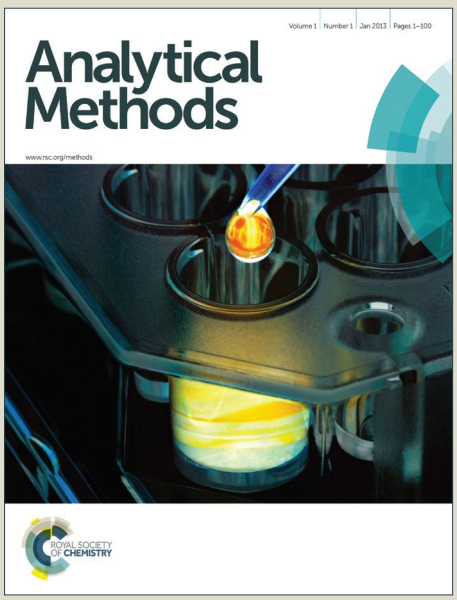

This is an *Accepted Manuscript*, which has been through the Royal Society of Chemistry peer review process and has been accepted for publication.

Accepted Manuscripts are published online shortly after acceptance, before technical editing, formatting and proof reading. Using this free service, authors can make their results available to the community, in citable form, before we publish the edited article. We will replace this *Accepted Manuscript* with the edited and formatted *Advance Article* as soon as it is available.

You can find more information about *Accepted Manuscripts* in the Information for Authors.

Please note that technical editing may introduce minor changes to the text and/or graphics, which may alter content. The journal's standard Terms & Conditions and the Ethical guidelines still apply. In no event shall the Royal Society of Chemistry be held responsible for any errors or omissions in this *Accepted Manuscript* or any consequences arising from the use of any information it contains.

ROYAL SOCIETY OF CHEMISTRY

www.rsc.org/methods

A novel electrochemical aptasensor based on MWCNTs-BMIMPF$_6$ and amino functionalized graphene nanocomposites film for determination of kanamycin

Xiaoli Qin,[a] Wenjuan Guo,[*a] Huijing Yu,[b] Juan Zhao,[a] and Meishan Pei[a]

[a]*Shandong Provincial Key Laboratory of Chemical Sensing & Analysis, School of Chemistry and Chemical Engineering, University of Jinan, Jinan 250022, China.*

[b]*Wen Deng Osteopath Hosptial of Shandong Province, Weihai 264400, China.*

[*] Corresponding author. Tel: +86-15689733522;

E-mail: chm_guowj@163.com.

Abstract

A simple electrochemical sensor based on a novel composite film consisting of multi-walled carbon nanotubes (MWCNTs), a room temperature ionic liquid (RTIL) of 1-butyl-3-methylimidazolium hexafluorophosphate ($BMIMPF_6$), and amino functionalized graphene (GR-CO-NH-CH_2-CH_2-NH_2) was constructed for the detection of kanamycin. Firstly, MWCNTs-$BMIMPF_6$ composites were fabricated on the surface of a glass carbon electrode (GCE). The synergy mechanism between MWCNTs and RTIL has been discussed. Secondly, GR-CO-NH-CH_2-CH_2-NH_2 was modified on the first film, which could greatly improve the conductivity of the electrode. The structure of the resultant graphene oxide (GO) was confirmed by FTIR and SEM. The properties of the aptasensor were characterized by the electrochemical methods. Under the optimum conditions, the electrochemical aptasensor exhibited a wide linear range for kanamycin from 0.001 to 100 μM with a low limit of detection of 0.87 nM (S/N=3). The as-prepared aptasensor showed high sensitivity, reproducibility and stability. Finally, the proposed electrochemical aptasensor was successfully applied for the detection of kanamycin in a real sample.

Keywords: Aptasensor; Ionic liquid; Multi-walled carbon nanotubes; Graphene; Kanamycin

Introduction

Kanamycin is a kind of important aminoglycoside antibiotic[1-3] produced by the fermentation of streptomyces kanamyceticus[4]. It is widely used in veterinary medicines to inhibit the growth of both Gram-positive and Gram-negative bacteria[5,6]. However, kanamycin can be accumulated in human body through food chain, which may result in serious side effects, such as loss of hearing, toxicity to the kidneys, and allergic reactions to the drugs[7-11]. Therefore, it is critical to detect kanamycin in food products in order to avoid exceeding intake of kanamycin[12,13]. European Union (EU) has estabilished maximum residue limits (MRLs) for kanamycin in edible tissues and milk: 100 μg kg^{-1} for meat, 600 μg kg^{-1} for liver, 2500 μg kg^{-1} for kidney, and 150 μg kg^{-1} for milk.

Recently, many analytical methods, such as colorimetric technique[14-18], enzyme-linked immunosorbent assay (ELISA)[19], chemiluminescence assay[20], fluorescence assay[21-23] and electrochemical immunoassay[24], have been reported for the detection of kanamycin. Yu et al. [9], Zhao et al. [25] and Wei et al. [26] reported the label-free immunosensors for the detection of residual kanamycin in animal derived foods. Kitagawa et al. [27], Loomans et al. [28] and Jin et al. [29] reported the development of the effective methods for determining kanamycin in serum or milk. The techniques mentioned above can be used to detect residual kanamycin, while they are usually time-consuming, complicated and expensive.

Recently, the most popular method for detecting kanamycin is ELISA[30,31]. Although ELISA is a powerful tool for the detection of antibiotics in food, it involves

numerous incubation, wash steps and expensive instruments[32]. In comparison with the ELISA method, electrochemical aptasensor has attracted increasing research interest due to its advantages of improved sensitivity, shortened analysis time, simplified operations, low cost, high stability and reproducibility [33-35].

Aptamers, the synthetic single-stranded DNA or RNA molecules with specific 3D structures, are selected through systematic evolution of ligands by exponential enrichment (SELEX) [4]. They can recognize and bind to a variety of target molecules including small molecules and organisms[36-38]. Aptamers have numerous advantages over the traditional recognition elements, such as antibodies and enzymes[39]. Therefore aptamers have provided the potential method for the fast and convenient detection of the residual kanamycin.

To further improve the sensitivity of the sensor for kanamycin, the electrode has been modified with the nanocomposites. Carbon nanotubes (CNTs)[40-42] have been widely used as the common nanomaterial for analytical applications. However, CNTs tend to aggregate into entangled networks or packed ropes through strong π-π stacking interactions[42-44]. Therefore, it is necessary to find an ideal media to improve the dispersity of CNTs. It is found that CNTs could be easily untangled into much finer bundles in RTIL[40-42]. Moreover, CNTs-IL composites[45,46] have been widely used as an effective load matrix which could enhance the current response significantly. At present, the surface functionalization of GR [47] has been widely applied to modify the electrodes and can avoid the agglomeration.

In this work, a novel aptasensor for the detection of kanamycin was fabricated by utilizing multi-walled carbon nanotubes (MWCNTs)-1-butyl-3-methylimidazolium hexafluorophosphate ($BMIMPF_6$) (MWCNTs-$BMIMPF_6$) and amino functionalized graphene (GR-CO-NH-CH_2-CH_2-NH_2) as the matrix. MWCNTs-$BMIMPF_6$ composites provided a smoothly conductive pathway for electron transfer, but there are seldom reports about its application in electrochemical aptasensor to detect the residual kanamycin. The as-prepared aptasensor showed a wide linear range for kanamycin from 0.001 to 100 μM with a low detection limit of 0.87 nM (about 0.507 ng/mL). The prepared aptasensor showed high sensitivity, reproducibility and stability. In this article, we performed a controlled trial by a reference ELISA method for determining kanamycin in milk. In view of these merits, we reported a facile and rapid electrochemical aptasensor and with low cost for sensitive detection of residual kanamycin. Thus, the proposed electrochemical aptasensor may have potential applications for detecting residual kanamycin in the field of food analysis.

2. Materials and methods

2.1. Materials

MWCNTs were obtained from Beijing Dekedaojin technology Co., Ltd. (China). $BMIMPF_6$ was obtained from Sigma-Aldrich (St. Louis, USA). Graphite was obtained from Jingchun Co., Ltd. (Shanghai, China). Ethanediamine (En), EDC, NHS, chitosan (CS), kanamycin sulfate, tryptamine, folic acid, DL-typtophan, glucose were purchased from Aladdin Co. Ltd (Beijing, China). Kanamycin selective aptamer modified with phosphate group at the 5’ position, namely

5'-PO_4-AGATGGGGGTTGAGGCTAAGCCGA-3' was synthesized by Beijing Genomics Institute (Beijing, China). All other chemicals were of analytical grade and received from Sinopharm Chemical Reagent Co., Ltd. (Beijing, China). Double distilled water was used throughout the experiments.

2.2. Apparatus

CV and DPV measurements were performed with a CHI 760E electrochemical workstation (Chenhua Instruments Co., Shanghai, China). EIS was carried out with Zennium electrochemical workstation (Zahner, Germany). A three-electrode system was consisted of a modified glassy carbon working electrode (GCE), a platinum wire counter electrode and a KCl saturated Ag/AgCl reference electrode. All electrochemical measurements were operated at RT. The FTIR spectrum was measured on Nicolet Avatar 370 DTGS (Nicolet, USA). Scanning electron micrographs (SEM) were obtained by a QUANTA PEG 250 microscope.

2.3. Synthesis of the graphene oxide

The graphene oxide (GO) was prepared based on a reported method[48]. Firstly, a mixture of graphite powders and $KMnO_4$ were added to a mixture of H_2SO_4 and H_3PO_4 (v/v=9:1), which caused the temperature slightly increased to 35-40 ℃. Then the mixture was heated to 50 ℃ and stirred overnight. The reaction was cooled to RT and poured onto ice (400 mL) with 30% H_2O_2 (3 mL). After that, the mixture was centrifuged at 4000 rpm for 20 min and the supernatant was decanted away. The solid material was washed with HCl, ethanol, and ultrapure water until the pH of

supernatant was neutral. The achieved graphite oxide was dried overnight. Graphite oxide powder was dispersed in ultrapure water by ultrasonication for 1 h and subsequently centrifuged for 15 min at 3000 rpm and dried overnight. GO was synthesized successfully.

2.4. Fabrication of the aptasensor

GCE was polished with 0.3 and 0.05 μm alumina powder and then washed thoroughly with ethanol and ultrapure water. Then, 5 μL of MWCNTs-$BMIMPF_6$ composites were dropped onto the electrode surface. MWCNTs-$BMIMPF_6$ composites were prepared according to the literature[42]. Next, 5 μL of GO/CS (V_{GO}: V_{CS}=4:1, C_{GO}=1 mg/mL) was deposited onto the MWCNTs-$BMIMPF_6$ modified electrode surface. Then the electrode was immersed in 1mL hydrazine and heated to 60 ℃ for 6 h. The electrode was rinsed thoroughly with 0.1 M phosphate buffer solution (PBS, pH=7.4). GR/MWCNTs-$BMIMPF_6$ modified electrode was obtained. Subsequently, the modified electrode was carboxylated for 5 min at 1.5 V in PBS and then soaked in EDC/NHS solution (pH=6) for 12 h to activate the introduced carboxyl groups of GR. Then, the electrode was allowed to react with En (67 mg/mL) by covalent bind in order to introduce the amino group into the GR-COOH/MWCNTs-$BMIMPF_6$ electrode. The modified working electrode was immersed in PBS containing 1.628 μM kanamycin aptamer and 10 mM EDC/NHS for 6 h. Then the electrode was washed several times with PBS to remove the unbound aptamer. Finally, the modified electrode was incubated in a varying concentration of kanamycin solutions for 2 h. The as-prepared electrodes were stored at 4 ℃ before used.

2.5. Electrochemical measurements

All electrochemical measurements including CV, EIS and DPV were carried out in a conventional three-electrode electrochemical cell. DPV was operated in 0.1 M PBS (pH=7.4) containing 5.0 mM $K_3[Fe(CN)_6]$ and 0.2 M KCl. EIS was recorded in 0.1 M PBS containing 0.2 M KCl and 5.0 mM $K_3[Fe(CN)_6]/K_4[Fe(CN)_6]$. DPV was recorded within the potential range from -0.2 to +0.6 V with a modulation amplitude of 0.05 V, a pulse width of 0.05 s and sample width of 0.0167 s.

3. Results and discussion

3.1. Scheme of electrochemical aptasensor

Scheme 1 displays the fabrication procedure of the proposed aptasensor. Firstly, MWCNTs-$BMIMPF_6$ was fabricated on the GCE surface, which combined the advantages of MWCNTs and RTIL. Secondly, GO/CS was coated on the surface of MWCNTs-$BMIMPF_6$ followed by reduction with hydrazine to obtain a GR/MWCNTs-$BMIMPF_6$ coated electrode. Then, the modified electrode was carboxylated for 5 min at 1.5 V. The obtained GR-COOH/MWCNTs-$BMIMPF_6$ electrode was activated with EDC and NHS. Subsequently, En was immobilized onto GR-COOH/MWCNTs-$BMIMPF_6$ electrode surface by an amidation reaction between the carboxyl groups of GR and the amino groups of En. Finally, kanamycin aptamer was connected to the modified electrode through the formation of phosphoramidate bond between the introduced amino group of GR and the phosphate group of the aptamer at 5' end[49,50]. Results showed that

MWCNTs-BMIMPF$_6$/GR-CO-NH-CH$_2$-CH$_2$-NH$_2$ composites were successfully designed as a sensitive aptasensor platform for kanamycin determination. In this article, phosphoramidate bond, a kind of covalent bond, was applied to improve the stability of aptasensor. It has a strong force similar to Au-NH[5] or Au-S bond. They have the potential application instead of the traditional Au-NH or Au-S bond due to its low-cost.

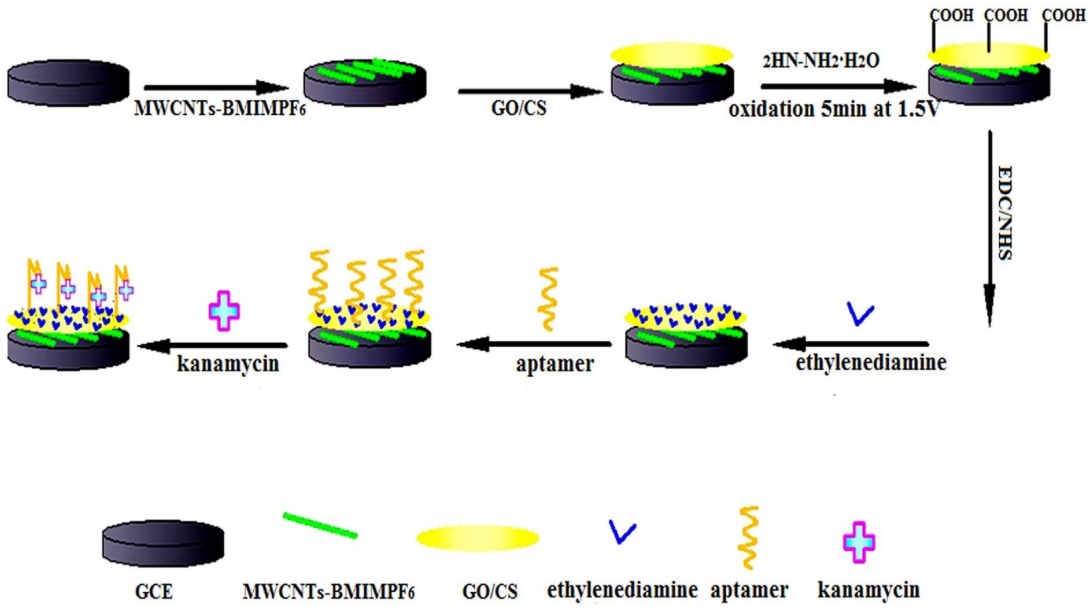

Scheme 1 Schematic illustration of the aptasensor for the detection of kanamycin.

3.2. Characterization of GO

The obtained GO was characterized by FTIR spectra and SEM. As shown in Fig. 1A, compared with the FTIR spectrum of graphite (curve a), the specific peaks appeared on the spectrum of GO (curve b), such as –OH (~3428 cm^{-1}), C=O (1722 cm^{-1}), C=C (1627 cm^{-1}) and epoxy (1230, 1060 cm^{-1}), which confirmed the successful oxygen of the graphite and the presence of large amounts of carboxyl groups on the surface of GO[51,52]. Furthermore, the SEM image further supplied the evidence of the

surface morphology of GO (Fig. 1B). SEM micrograph proved that the synthesized GO consisted of many cavities, stacked and crumpled flakes closely associated with each other.

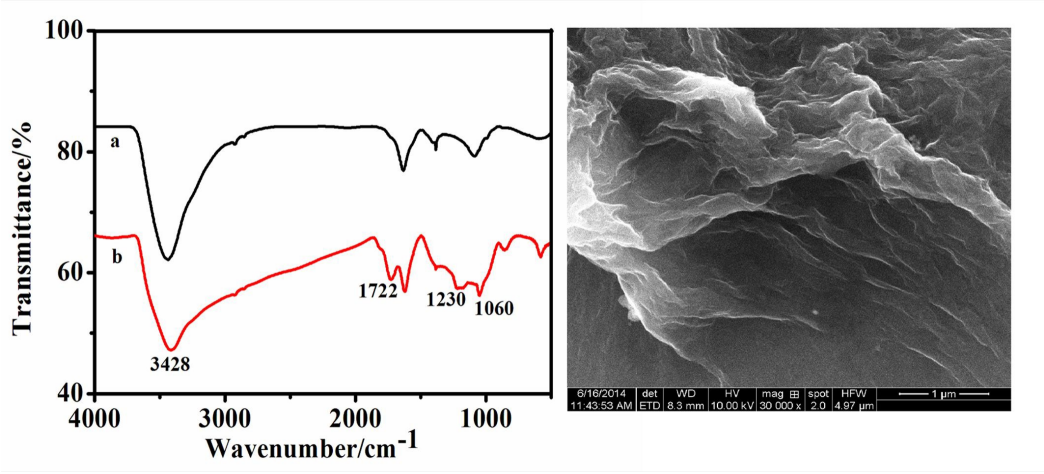

A **B**

Fig. 1 (A) FTIR spectrum of graphite (a) and GO (b). (B) SEM image of GO.

3.3. Electrochemical characterization of the modified electrodes

CV is an effective and convenient method for probing the feature of the different electrodes. As shown in Fig. 2A, the bared GCE had a pair of redox peaks (curve a), indicating a reversible electrochemical process. It is noticeable that the MWCNTs-$BMIMPF_6$ composites modified electrode caused larger redox peak currents (curve c) than that of the MWCNTs modified electrode (curve b), which indicated that the presence of $BMIMPF_6$ could improve the dispersion of MWCNTs and enhance the conductivity of the electrode. The introduction of MWCNTs-$BMIMPF_6$ could increase the effective area of the electrode. After MWCNTs-$BMIMPF_6$/GCE was modified with GR-COOH (curve d), there was a

significantly increased current peaks in the CV curve, which indicated that GR greatly promoted the electron transfer, due to its excellent electrical conductivity. Curve e and f showed that En and aptamer were immobilized on the surfaces of the modified electrodes. The aptamer/GR-CO-NH-CH_2-CH_2-NH_2/MWCNTs-$BMIMPF_6$/GCE showed a weaker CV signal in contrast with the GR-CO-NH-CH_2-CH_2-NH_2/MWCNTs-$BMIMPF_6$/GCE, suggesting that aptamer formed an isolating layer and blocked the electron transfer of the redox probe. After the incubation with kanamycin, the formation of the aptamer-kanamycin complex hindered the interfacial electron transfer to the modified electrode surface and resulted in a further decrease in peak current (curve g). MWCNTs-$BMIMPF_6$ composites played an important role in enhancing the capability of electron transfer and the introduction of GR-CO-NH-CH_2-CH_2-NH_2 could bring about a sensitive electrode substrate, which was believed to be a new idea for the construction of simple and powerful electrochemical aptasensor.

EIS is one of the most powerful tools for studying the characteristics of the modified electrodes. In order to gain insight into the fabrication process of the aptasensor, Fig. 2B shows the Nyquist plots of different modified electrodes. In EIS, the semicircle diameter equals the charge-transfer resistance (R_{ct}). The EIS of the bared GCE (curve a) showed a relatively larger resistance. It was easy to find that the R_{ct} of the MWCNTs/GCE (curve b) was higher than that of MWCNTs-$BMIMPF_6$ modified GCE (curve c), suggesting the synergic effect of MWCNTs and $BMIMPF_6$ could improve the electron transfer process on the surface of sensor. When

GR-COOH was coated on the MWCNTs-BMIMPF$_6$/GCE surface, a smaller electron transfer resistance (curve d) was obtained, suggesting that GR-COOH could promote the electrochemical response. When the GR-CO-NH-CH$_2$-CH$_2$-NH$_2$/MWCNTs-BMIMPF$_6$ nanocomposites were immobilized, the resistance of the electrode increased remarkably (curve e), indicating that the modified MWCNTs-BMIMPF$_6$/GR-CO-NH-CH$_2$-CH$_2$-NH$_2$ film hindered the electron transfer. At last, the capture of aptamer and kanamycin molecules blocked the electron exchange between the redox probe and the electrode, and led to further increase of resistance (curve f and curve g). Results showed that the aptamer and kanamycin were successively assembled onto the modified electrode surface. It was confirmed that the EIS results were agreed with those of the CVs in Fig 2A.

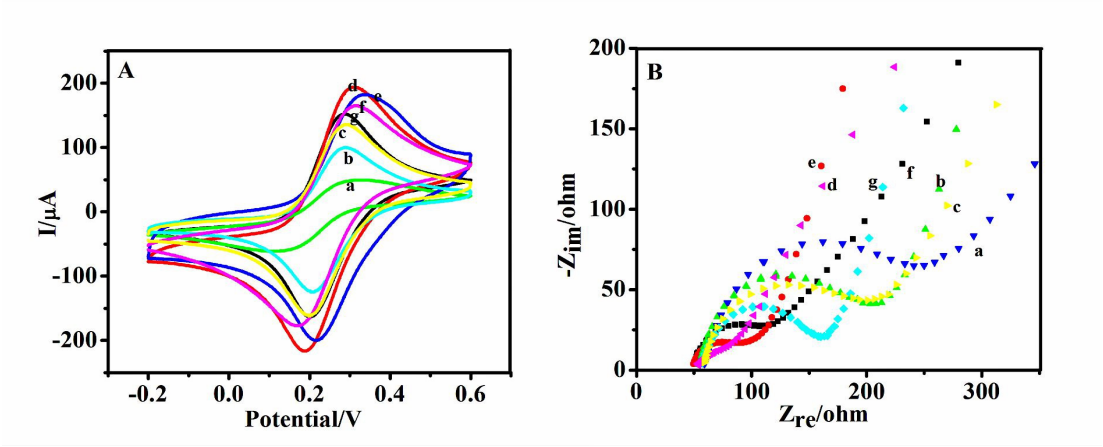

Fig. 2 (A) CVs of (a) bare GCE; (b) MWCNTs/GCE; (c) MWCNTs-BMIMPF$_6$/GCE; (d) GR-COOH/MWCNTs-BMIMPF$_6$/GCE; (e) GR-CO-NH-CH$_2$-CH$_2$-NH$_2$/MWCNTs-BMIMPF$_6$/GCE (f) aptamer/GR-CO-NH-CH$_2$-CH$_2$-NH$_2$/MWCNTs-BMIMPF$_6$/GCE; (g) kanamycin/aptamer/GR-CO-NH-CH$_2$-CH$_2$-NH$_2$/MWCNTs-BMIMPF$_6$/GCE; Scan rate: 100 mV/s. (B) Nyquist diagrams of electrochemical impedance spectra recorded

form 0.1 to 10^5 Hz. The modified electrodes are the same as (A).

To further confirm the above speculation, the electroactive surface areas (A) of the four kinds of electrodes were calculated based on the Randles–Sevcik equation[42]:

$$Ip=2.65\times10^5n^{3/2}AD^{1/2}\upsilon^{1/2}C$$

where Ip is the peak current, n is the transferring electron number, A is the electroactive area (cm^2), D is the diffusion coefficient, υ is the scan rate and C is the concentration of the substrate. The diffusion coefficient of $K_3[Fe(CN)_6]$[50] is 7.6×10^{-6} cm^2 s^{-1}. The calculated results are revealed in Table 1. Results showed that the electroactive areas were calculated to be 0.0688 cm^2, 0.291 cm^2, 0.415 cm^2 for GCE, MWCNTs-$BMIMPF_6$/GCE and GR-CO-NH-CH_2-CH_2-NH_2/MWCNTs-$BMIMPF_6$/GCE, respectively. The electroactive surface area of the GR-CO-NH-CH_2-CH_2-NH_2 deposited on the MWCNTs-$BMIMPF_6$/GCE was larger than that of other modified electrodes, which further proved that A was increased obviously after electrode modification. MWCNTs bundles could be considerably untangled within $BMIMPF_6$, greatly increasing the effective area of the electrode.

Table 1 The electroactive surface area (A) of different modified electrodes.

Electrode	A(cm^2)
GCE	0.0688
MWCNTs/GCE	0.184
MWCNTs-$BMIMPF_6$/GCE	0.291
GR-CO-NH-CH_2-CH_2-NH_2/MWCNTs-$BMIMPF_6$/GCE	0.415

3.4. Characteristics of the SEM

The morphologies of the different modified electrodes were characterized by

SEM. As is shown in Fig. 3, MWCNTs were well distributed on the surface of the GCE with the formation of much finer bundles in the presence of $BMIMPF_6$ (Fig. 3a). [$BMIM^+$] (Fig. 4) consists of imidazole ring and alkyl chain. The imidazole ring possesses a π-conjugated structure, and positive charge mainly localized in imidazole ring[42]. π-Electron and cation in $BMIMPF_6$ could interact with the π-electron in MWCNTs. When the MWCNTs and $BMIMPF_6$ were mixed, the high surface energy of the detached MWCNTs was effectively appeased via strong π-π stacking interactions and weak "cation–π" [53] interactions between the MWCNTs and $BMIMPF_6$. Thus, $BMIMPF_6$ played an important role in dispersing MWCNTs. From Fig. 3b, the SEM image reveals that the surface morphology of GR-CO-NH-CH_2-CH_2-NH_2/MWCNTs-$BMIMPF_6$ was significantly different from that of MWCNTs-$BMIMPF_6$ and bright regions could be obviously observed, which suggested that GR-CO-NH-CH_2-CH_2-NH_2 has been successfully modified on MWCNTs-$BMIMPF_6$ surface. After the immobilization of aptamer (Fig. 3c), irregular structure appeared onto the GR-CO-NH-CH_2-CH_2-NH_2/MWCNTs-$BMIMPF_6$ surface that confirmed the attachment of aptamer onto the modified electrode surface. According to the SEM, it can be demonstrated that the modification of the electrode was constructed successfully.

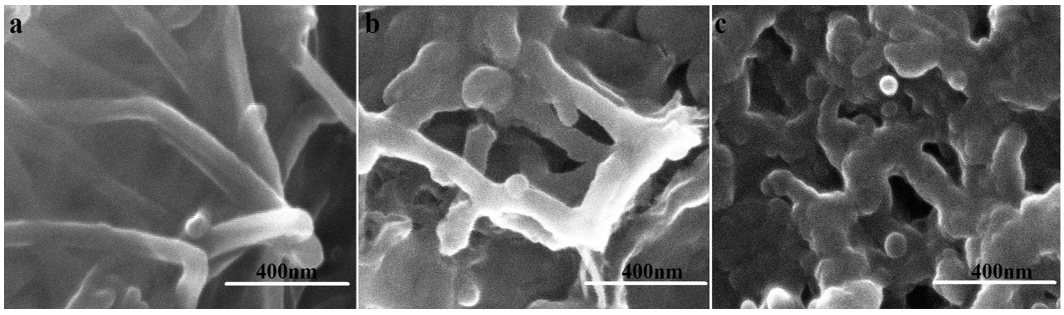

Fig. 3 SEM images of (a) MWCNTs-$BMIMPF_6$/GCE (b) GR-CO-NH-CH_2-CH_2-NH_2/MWCNTs-$BMIMPF_6$/GCE and (c) aptamer/GR-CO-NH-CH_2-CH_2-NH_2/MWCNTs-$BMIMPF_6$/GCE.

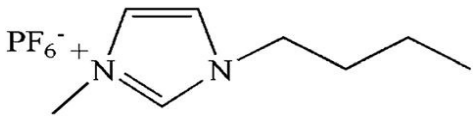

Fig. 4 Structure of $BMIMPF_6$.

3.5. Optimization of experimental conditions

In order to achieve maximum electrochemical response of the aptasensor, experimental parameters were optimized in terms of the mass ratio of $BMIMPF_6$ and MWCNTs, the pH of PBS in the detection of kanamycin and the incubation time of kanamycin. The mass ratio of $BMIMPF_6$ and MWCNTs was investigated and the corresponding results are shown in Fig. 5A. It's obvious that the highest value of electrochemical response was achieved at 1:0.08 among different ratios ranging from 1:0.04 to 1:0.12. When the ratio of $BMIMPF_6$ and MWCNTs ranged from 1:0.04 to 1:0.12 with the increase of MWCNTs, more and more MWCNTs with good conductivity enhanced the current signal. Further increasing the amount of MWCNTs, namely the ratio of $BMIMPF_6$ and MWCNTs beyond 1:0.08, the current signal decreased on the contrary. Over the ratio of 1:0.08, MWCNTs were excessive and could not be dispersed entirely in $BMIMPF_6$. The reason was ascribed to the solvent effect of IL. In the presence of $BMIMPF_6$, MWCNTs were detached from the bundles under the action of shear force and $BMIMPF_6$ could keep the detached MWCNTs from rebinding together again under the effect of shielding the π-π stacking

interaction between MWCNTs. If there was too much $BMIMPF_6$, the MWCNTs could be wrapped up by $BMIMPF_6$, so as to counteract the advantage of the MWCNTs. Therefore, $BMIMPF_6$ played an irreplaceable role in the process of dispersing MWCNTs.

The effect of PH was investigated by recording DPV of the modified electrode in PBS with PH values ranging from 6.2 to 8.2. As shown in Fig. 5B, the DPV response continued to increase until pH was up to 7.4, and then decreased over pH 7.4. The optimal current response was obtained at pH 7.4, indicating that the aptamer could not combine well with kanamycin in strong acidic and alkaline solutions. Therefore, pH 7.4 was chosen as the optimal pH for determination of kanamycin.

The incubation time of kanamycin is an important parameter for the performance of aptasensor to achieve maximized current signal. The relationship between the sensor response and the incubation time is shown in Fig. 5C. The DPV signal increased continually with increasing of the incubation time from 10 to 120 min and was inclined to level off when the incubation time was 120 min because of the saturation of the active sites for kanamycin binding. Thus, the incubation time of 120 min was chosen as an optimal condition for the determination of kanamycin.

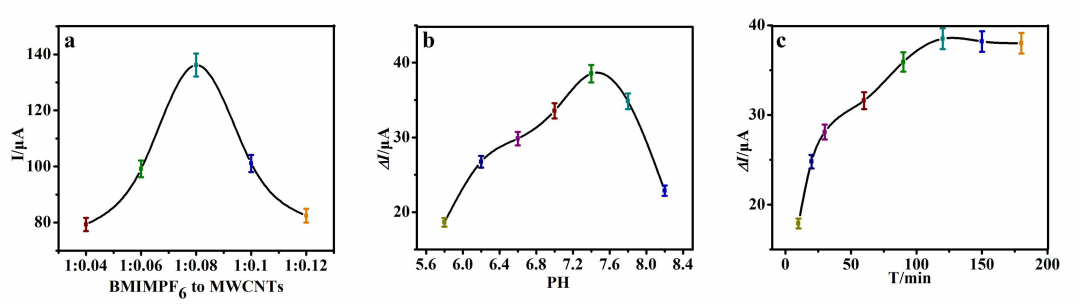

Fig. 5 Effect of (a) the mass ratio of $BMIMPF_6$ to MWCNTs on the CV peak current

of the aptasensor; (b) the value of pH and (c) the incubation time of kanamycin on the DPV peak current of the aptasensor.

3.6. Calibration curve of the aptasensor

Under the optimum conditions, the aptasensors were incubated in different concentrations of kanamycin and the DPV responses of the proposed aptasensors were recorded. As shown in the inset of Fig. 6, the DPV current decreased gradually with increasing of kanamycin concentration. The corresponding calibration curve exhibited a good linear relationship with kanamycin concentration over the range of 0.001-100 μM with the limit of detection of 0.87 nM (about 0.507 ng/mL) at a signal-to-noise ratio of 3 (Fig. 6). The linear equation could be fitted as △I (μA) =17.64519+3.46013c (μM) (R^2=0.9992). The limit of detection of as-prepared aptasensor is comparably highly sensitive to those of previously reported oligonucleotide-based luminescent[8] (83.3 ng/mL), gold-nanoparticle-based colorimetric[18] (15 ng/mL), ELISA[28] (12.2 ng/mL) and aptasensor[54] (5.2 ng/mL). Results of the proposed aptasensor for kanamycin was compared with that of the other reported methods in Table 2. The proposed aptasensor offered the advantages of wide linear range, shortened analysis time, simplified operations with no need of expensive instrumentation and consumption of large amount of reagent.

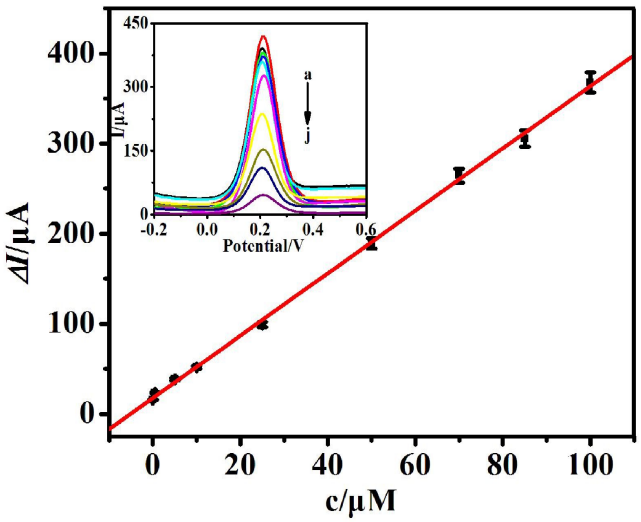

Fig. 6 Calibration curve of DPV peak currents for different kanamycin concentrations from 0.001 μM to 100 μM. The inset shows DPV responses of the electrochemical aptasensor to different concentrations of kanamycin (from a to j: 0, 0.001, 0.5, 5, 10, 25, 50, 70, 85, 100 μM).

Table 2 Comparison of kanamycin determinations using the proposed method and reference methods.

Methods	Reagents or condition	Linear range	Detection limit	Reference
Oligonucleotide-based luminescent assay	Luminescent platimum complex	0.2–150 μM	143 nM	8
Label-free cantilever array sensor	Cantilever array functionalization	100 μM-10 mM	50 μM	4
Colorimetric method	Gold nanoparticle	-	25 nM	18

Label-free immunosensor	Silver hybridized mesoporous ferroferric oxide	0.09-27 nM	0.03 nM	9
ELISA	-	-	4.15 nM	57
ELISA	-	-	21 nM	28
Label-free aptasensor	Functionalized Aptamer	0.05 μM-9 μM	9.4±0.4 nM	54
Fluorescence detection	Fluorescence method	27 nM-67 μM	25.6 nM-8.95 nM	56
Aptasensor detection	Gold nanoparticles	10 nM-0.15μM	5.8 nM	58
Label-free electrochemical immmunosensor	Nanoporous gold	0.03 nM-24 nM	0.01 nM	25
Fluorescence aptasensor	Upconversion nanoparticles	0.03-3 nM	18 pM	5
Electrochemical aptasensor	MWCNTs, $BMIMPF_6$, GR	0.001 μM-100 μM	0.87 nM	This work

Under optimum conditions, the proposed approach displayed high sensitivity for the determination of kanamycin, which was attributed to five factors. (1) $BMIMPF_6$ may not only be a good solvent but also improve the conductivity of electrochemical aptasensor. (2) The excellent film-forming ability, adsorption capability and

biocompatibility of CS might help the detection of kanamycin antibiotic. (3) The stability of MWCNTs-BMIMPF$_6$/GR-CO-NH-CH$_2$-CH$_2$-NH$_2$ nanocomposites was good and the aptamer could firmly be attached to the modified electrode surface through the formation of phosphoramidate bond between the introduced amino groups of the GR-CO-NH-CH$_2$-CH$_2$-NH$_2$ and phosphate groups of the aptamer at 5' end. (4) The good electron transfer ability of MWCNTs and GR resulted in the dual-amplification effects. (5) MWCNTs–BMIMPF$_6$ composites were used as an effective load matrix for the deposition of GR-CO-NH-CH$_2$-CH$_2$-NH$_2$, which could play a key role in improving the capability of electron transfer.

3.7. The reproducibility, repeatability, specificity and stability of the aptasensor

To evaluate the reproducibility of the aptasensor, five electrodes were prepared following the same procedure to determine a kanamycin solution of 5 μM. The relative standard deviation (RSD) was 3.9%, indicating the good reproducibility of the aptasensor.

To investigate the repeatability of the aptasensor, five electrodes were examined under the same conditions. After using the five electrodes for 5 times continuously, the RSD of 2.7% was observed, which indicated that the aptasensor had good repeatability.

Specificity is an important criterion for aptasensors to detect kanamycin. The current responses of the prepared aptasensor to kanamycin (5 μM), tryptamine, folic acid, DL-typtophan, glucose, mixtures of kanamycin (5 μM) and interfering

substances (10 μM) were studied. As shown in Fig. 7A, kanamycin showed a much stronger current response (Fig. 7a), in addition, mixtures of kanamycin and interference also showed a much stronger current response (Fig. 7f-i). Then, it was observed that weak current response in the presence of these interferents (Fig. 7b-e), indicating that kanamycin aptamer could only recognize kanamycin and could not combine with other biomolecules. All those results confirmed that the developed aptasensor had excellent selectivity.

To demonstrate the stability of the aptasensor, CV was measured for a 50-cycle successive scan and a 2.37% deviation of initial current response was observed (Fig. 7B), indicating that the fabricated aptasensor was sufficiently stable. To further test the stability of the aptasensor, a series of five electrodes prepared under the same conditions were utilized to detection 5 μM of kanamycin and stored at 4 ℃ before used. Results showed that current responses of the aptasensor retained 93% of the initial response after 2 weeks. The good stability of electrochemical aptasensor can be ascribed to two reasons: firstly, some biocompatible materials such as CS and RTIL had been introduced into the modified layers to improve the stability of the aptasensor. Secondly, the aptamer could be attached firmly to the working electrode surface.

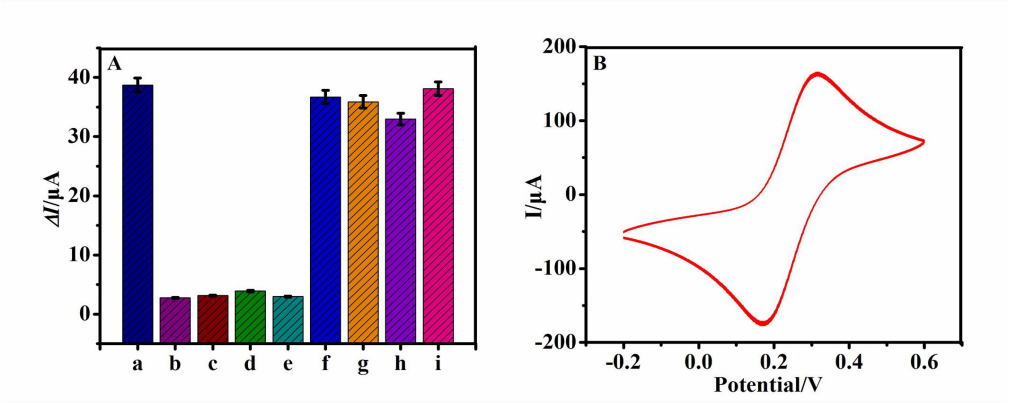

Fig. 7 (A) DPV current responses of the aptaensor to kanamycin (a), interferents (b-e), mixtures of kanamycin and interferents (f-i). Error bars are standard deviations across three repetitive experiments. (B) Stability analysis of the aptasensor.

3.8. Determination of kanamycin in real samples

Although the prepared aptasensor displayed excellent selectivity towards kanamycin, it is worthy to evaluate the feasibility of the proposed aptasensor in the practical application. It has attracted considerable attention to detection of kanamycin in milk. Milk is one of the most important regulated products in food industry due to the risk of having veterinary medicine residue[54,58]. Milk was diluted ten times with PBS. Then, kanamycin standard solution was spiked into the diluted milk to prepare the concentrations of kanamycin of 0.8, 1.0, 2.0, 5.0, 8.0 ng/mL. Finally, experiments were carried out under the optimized conditions. The calibration curve was obtained and the linear regression equation was expressed as: $\triangle$I (μA)= 21.0811+3.27153c (μM) (R^2=0.9987). The RSD was determined less than 3%. The detection limit of kanamycin in the milk sample was determined to be 0.943 nM (about 0.549 ng/mL), which was comparable or lower than the previously reported values[28,54-56]. Moreover, the detection limit was much lower than the maximum residue level of kanamycin in milk (150 ng/mL, about 257 nM) established by the European Union legislation. To further investigate the practical application of the aptasensor, we performed a controlled trial by a reference ELISA method. Results are listed in Table 3. It is found that the relative deviation between the two methods ranged from -1.61% to 6.04%, indicating that there is no significant difference between the electrochemical and

ELISA method. The kanamycin concentration recovery was in the range of 92.15% to 105.99% with RSDs below 4.0% for the milk sample. The recovery values of the electrochemical aptasensor were consistent with that of ELISA. This clearly demonstrated that the developed sensor could be successfully applied to detect kanamycin in milk sample.

Table 3 Comparison of kanamycin detection between the proposed aptasensor and ELISA method in kanamycin-spiked milk samples.

Kanamycin in milk (ng/mL)	Electrochemical detection (ng/mL ± RSD%)	Recovery (%)	ELISA method (ng/mL)	Relative deviation (%)
0.5	0.4812±2.91	96.24	0.49	-1.79
0.8	0.8479 ±2.78	105.99	0.81	4.68
1.0	0.9215 ± 3.57	92.15	0.9	2.39
5.0	4.8965 ± 3.09	97.93	4.8	2.01
8.0	8.3633 ± 2.52	104.54	8.5	-1.61

Conclusions

In this work, a simple and sensitive electrochemical aptasensor using MWCNTs-BMIMPF$_6$/GR-CO-NH-CH$_2$-CH$_2$-NH$_2$ as a sensor platform to sequentially immobilize kanamycin aptamer was successfully developed for kanamycin detection. The proposed aptasensor offered several advantages: (1) MWCNTs-BMIMPF$_6$ composites could increase the effective area of the electrode due to the synergy of the MWCNTs and RTIL. (2) MWCNTs-BMIMPF$_6$/GR-CO-NH-CH$_2$-CH$_2$-NH$_2$ nanocomposites greatly improved the conductivity of the aptasensor. (3) The electroactive surface area of the GR-CO-NH-CH$_2$-CH$_2$-NH$_2$/MWCNTs-BMIMPF$_6$/GCE was larger than that of other modified electrodes, which could enhance the immobilized quantity of kanamycin

aptamer. (4) The electrochemical aptasensor exhibited a wide linear range for kanamycin from 0.001 to 100 μM with a low detection limit of 0.87 nM, which exhibited higher sensitivity. (5) We performed a further controlled trial by a reference ELISA method in kanamycin-spiked milk samples. These data obtained using the proposed aptasensor were in good agreement with those obtained by utilizing ELISA. Under the optimized conditions, the proposed aptasensor showed high sensitivity, reproducibility and stability. The presented aptasensor was demonstrated to be simple and cost-efficient, which provided potential applications for kanamycin detection in the field of food analysis.

Acknowledgements

This work was supported financially by Shandong Provincial Natural Science Foundation, China (Grant No. ZR2012BL11 and ZR2011EMQ010), and Shandong Provincial Science and Technology Development Plan Project, China (Grant No. 2013GGX10705).

References

1 C. M. Spahn, C. D. Prescott, J. Mol. Med., 1996, 74, 423–439.

2 E. Goldman, Hum. Ecol. Risk Assess., 2004, 10, 121–134.

3 H. C. Wegener, Meat Sci., 2010, 84, 279–283.

4 X. J. Bai, H. Hou, B. L. Zhang, J. L. Tang, Biosens. Bioelectron., 2014, 56, 112-116.

5 H. Li, D.-E. Sun, Y. J. Liu, Z. H. Liu, Biosens. Bioelectron., 2014, 55, 149-156.

6 D. Fourmy, S. Yoshizawa, J. D. Puglisi, J. Mol. Biol, 1998, 277, 333-345.

7 R. Oertel, V. Neumeister and W. Kirch, J. Chromatogr. A., 2004, 1058, 197-201.

8 K.-H. Leung, H. Z. He, D. S.-H. Chan, W.-C. Fu, C.-H. Leung, D.-L. Ma, Sens. Actuators, B, 2013, 177, 487-492.

9 S. J. Yu, Q. Wei, B. Du, D. Wu, H. Li, L. G. Yan, H. M. Ma, Y. Zhang, Biosens. Bioelectron., 2013, 48, 224-229.

10 G. J. Kaloyanides, E. Pastoriza-Munoz, Kidney International, 1980, 18, 571–582.

11 I. Kitasato, M. Yokota, S. Inouye, M. Igarashi, Chemotherapy, 1990, 36, 155–168.

12 D. M. Kim, M. A. Rahman, M. H. Do, C. Ban, Y. B. Shim, Biosens. Bioelectron., 2010, 25, 1781-1788.

13 Y. J. Jin, J. W. Jang, C. H. Han, M. H. Lee, J. Vet. Sci., 2006, 7, 111-117.

14 M. N. Stojanovic, P. D. Prada, D.W. Landry, J. Am. Chem. Soc., 2001, 123, 4928–4931.

15 J. W. Liu, Y. Lu, Angew. Chem. Int. Ed. Engl., 2006, 45, 90–94.

16 J. Elbaz, B. Shlyahovsky, D. Li, I. Willner, Chem. BioChem, 2008, 9, 232–239.

17 Y. Du, B. L. Li, S. J. Guo, Z. X. Zhou, M. Zhou, E. K. Wang, S. J. Dong, Analyst, 2011, 136, 493–497.

18 K.-M. Song, M. Cho, H. H. Jo, K. Min, S. H. Jeon, T. S. Kim, M. S. Han, J. K. Ku, C. Ban, Anal. Biochem, 2011, 415, 175-181.

19 R. Freeman, E. Sharon, R. Tel-Vered, I. Willner, J. Am. Chem. Soc., 2009, 131, 5028–5029.

20 Y. Li, H. Qi, Y. Peng, J. Yang, Ch. Zhang, Electrochim. Commun, 2007, 9, 2571–2575.

21 C. Y. Zhang, L.W. Johnson, Anal. Chem., 2009, 81, 3051–3055.

22 J. P. Hilton, T. H. Nguyen, R. J. Pei, M. Stojanovic, Q. Lin, Sens. Actuators. A: Phys., 2011, 166, 241–246.

23 C. P. Ma, W. S. Wang, Q. Yang, C. Shi, L. J. Cao, Biosens. Bioelectron., 2011, 26, 3309–3312.

24 P. L. He, Z. Y. Wang, L. Y. Zhang, W. J. Yang, Food Chem, 2009, 112, 707-714.

25 Y. F. Zhao, Q. Wei, C. X. Xu, H. Li, D. Wu, Y. Y. Cai, K. X. Mao, Z. T. Cui, B. Du, Sens. Actuators, B, 2011, 155, 618-625.

26 Q. Wei, Y. F. Zhao, B. Du, D. Wu, H. Li, M. H. Yang, Food Chem, 2012, 134, 1601-1606.

27 T. Kitagawa, K. Fujiwara, S. Tomonoh, K. Takahashi, M. Koida, J. Biochem, 1983, 94, 1165-1172.

28 E. E. M. G. Loomans, J. Wiltenburg, M. Koets and A. Amerongen, J. Agric. Food Chem., 2003, 51, 587-593.

29 Y. Jin, J.-W. Jang, C.-H. Han, M.-H. Lee, J. Vet. Sci., 2006, 7, 111-117.

30 Y. Q. Chen, Z. Q. Wang, Z. H. Wang, S. S. Tang, Y. Zhu, X. Xiao, J. Agric. Food Chem. 2008, 56, 2944-2952.

31 C. Chafer-Pericas, A. Maquieira, R. Puchades, 2010, 29, 1038-1049.

32 Y. P. Chen, M. Q. Zou, C. Qi, M.-X. Xie, D.-N. Wang, Y.-F. Wang, Q. Xue, J.-F. Li, Y. Chen, Biosens. Bioelectron., 2013, 39, 112-117.

33 G. S. Bang, S. Cho, B. G. Kim, Biosens. Bioelectron., 2005, 21, 863–870.

34 H. M. So, K. Won, Y. H. Kim, B. K. Kim, B. H. Ryu, P. S. Na, H. Kim, J. O. Lee, J. Am. Chem. Soc., 2005, 127, 11906–11907.

35 K. Maehashi, T. Katsura, K. Kerman, Y. Takamura, K. Matsumoto, E. Tamiya, Anal. Chem., 2007, 79, 782–787.

36 C. Tuerk, L. Gold, Science, 1990, 249, 505–510.

37 A. D. Ellington, J. W. Szostak, Nature, 1990, 346, 818–822.

38 C. L. A. Hamula, J. W. Guthrie, H. Zhang, X. F. Li, X. C. Le, Anal. Chem., 2006, 25, 681–691.

39 A. N. Kawde, M. C. Rodriguez, T. M. H. Lee, J. Wang, Electrochem. Commun, 2005, 7, 537–540.

40 M. Arvand, A. Niazi, R. Motaghed Mazhabi, P. Biparva, Journal of Molecular Liquids, 2012, 173, 1–7.

41 L. Zheng, J.-Q. Zhang, J.-F. Song, Electrochimica Acta, 2009, 54, 4559-4565.

42 W. J. Guo, Y. M. Liu, X. Meng, M. S. Pei, J. P. Wang, L. Y. Wang, RSC Adv. 2014, 4, 57773-57780.

43 T. Fukushima, A. Kosaka, Y. J. Ishimura, T. Yamoamoto, T. Takigawa, Science, 2003, 3000, 2072-2074.

44 J. C. Ma and D. A. Dougherty, Chem. Rev., 1997, 97, 1303-1324.

45 Y. H. Li, X. S. Liu, X. Y. Liu, N. N. Mai, Y. D. Li, W. Z. Wei, Q. Y. Cai, Colloids Surf. B, 2011, 88, 402-406.

46 X. L. Niu, W. Yang, H. Guo, J. Ren, J. Z. Gao, Biosens. Bioelectron., 2013, 41, 225-231.

47 F. L. Li, Y. M. Guo, X. Sun, X. Y. Wang, European food research and technology, 2014, 239, 227-236.

48 N. Pan, D. Guan, Y. Yang, Z. Huang, R. Wang, Y. Jin, C. Xia, Chem. Eng. J., 2014, 236, 471–479.

49 S. Liu, X. R. Xing, J. H. Yu, W. J. Lian, J. Li, M. Cui, J. D. Huang, Biosens. Bioelectro., 2012, 36, 186-191.

50 Y. Bo, H. Y. Yang, Y. Hu, T. M. Yao, S. S. Huang, Electrochimica Acta, 2011, 56, 2676-2681.

51 S. Stankovich, R. D. Piner, S. T. Nguyen, Carbon, 2006, 44, 3342-3347.

52 K.-J. Huang, D.-J. Niu, J.-Y. Sun, C.-H. Han, Z.-W. Wu, Y.-L. Li, X.-Q. Xiong, Colloids Surf. B., 2011, 82, 543-549.

53 T. Fukushima and T. Aida, Chem.-Eur. J., 2007, 13, 5048-5058.

54 Y. Zhu, P. Chandra, K.-M. Song, C. Ban, Y.-B, Shim, Biosens. Bioelectron., 2012, 36, 29-34.

55 S. R. Raz, M. G. E. G. Bremer,W. Haasnoot, W. Norde, Anal. Chem., 2009, 81, 7743–7749.

56 C. Z. Yu, Y. Z. He, G. N. Fu, H. Y. Xie and W. E. Gan, J. Chromatogr., B: Anal. Technol. Biomed. Life Sci., 2009, 877, 333–338.

57 H. Watanabe, A. Satake, Y. Kido, A. Tsuji, Analyst, 1999, 124, 1611-1615.

58 X. Sun, F. L. Li, G. H. Shen, J. D. Huang and X. Y. Wang, Analyst, 2014, 139, 299-308.